Ensemble Deep Spectrum Sensing in CRNs Co-existing with OFDM-based Networks

Mohammad Reza Amini, *Senior Member, IEEE,* Ala'a Al-Habashna, *Member, IEEE,* Gabriel Wainer, *Senior Member, IEEE*, and Gary Boudreau, *Senior Member, IEEE*

***Abstract*—We propose a novel machine learning-based architecture for smart sensing of the spectrum for Cognitive Radio (CR) networks. A Multi-resolution Correlation Deep Sensing Network (MrCorr-DSNet) is designed to extract signal energy and Cyclic Prefix (CP) similarities in OFDM-based signals as well as other non-explainable spatial-temporal features to enrich the extracted information needed for PU occupancy classification. By forming a 3D matrix for each observation vector using In-phase (I) an Quadrature (Q) samples in multi-antenna system, MrCorr-DSNet can fully exploit the temporal-spatial correlations with 3D CNNs. Furthermore, by adopting ensemble learning for several MrCorr-DSNets trained for different Signal-to-Noise Ratio (SNR) sub-ranges, the performance is significantly enhanced and the SNR-wall problem is resolved due to the synergy between weak and strong learners. The performance of the proposed structure is shown in terms of Receiver Operating Characteristics (ROC), confusion matrix, Area Under Curve (AUC), P-value, loss and the detection probability.**

***Index Terms*—Internet-of-Things, Latency, NOMA, Random Access, Reliability.**

I. Introduction

THE demand for radio spectrum has been contagiously growing due to the emergence of new wireless technologies, such as the Internet of Things, Cyber-Physical Systems, etc. This increase in demand is becoming a serious challenge since the spectrum is a limited resource. This scarcity has made the spectrum an invaluable asset. However, research has shown that licensed radio spectrum is under-utilized by the traditional ways of spectrum assignment. [1].

To efficiently utilize the spectrum, Dynamic Spectrum Access (DSA) under the concept of Cognitive Radio (CR) has been proposed [2]. This concept allows the Secondary Users (SUs) to opportunistically access the licensed band of the Primary User (PU). To this aim, SUs have to detect the presence of PU by sensing the spectrum in order to access the spectrum without interfering with the PU [3], [4]. Therefore, the performance of Spectrum Sensing (SS) directly affects the performance of co-existence between networks since misdetection of a PU will result in a SU attempting to use the spectrum during PU's transmission [5], causing interference with the licensed users. Hence, designing a robust spectrum sensing module with high detection performance is vital in CR systems. Many SS methods have been proposed in the literature. Generally speaking, SS has been classified into two main categories, blind SS and non-blind SS. Cyclostationary feature detection [6]–[8] and matched filter detection [9] are the main examples of non-blind SS which exploit the signal information to detect it. Blind methods are of interest as they do not need any prior information of the PU signal. They include Energy Detection (ED) [10], [11], Phase type model [12] Maximum Eigenvalue Detection (MED) [13], and Covariance Absolute Value (CAV) [14]. Such techniques have shown their advantages over decades. However, since they are model-based, they need some environmental information in their models such as statistical noise distribution to operate optimally. Therefore, they suffer from mismatches between estimated model and real life model which causes performance degradation.

Recently, Deep Learning (DL) has been increasingly applied in the area of signal processing [15]–[17]. DL has been also exploited in SS recently. As an example, [18] used Convolutional Neural Networks (CNNs) to detect PU signal. The authors proposed a covariance matrix-aware CNN (CM-CNN)-based spectrum sensing in which sample covariance matrix is fed as input to a CNN for signal detection. The results show that the performance of the proposed method is very close to that of optimal detector. A Stacked Autoencoder- based spectrum sensing (SAE-SS) method was designed in [19] to extract features from PU signal. To improve the detection performance, The authors used time-frequency domain signals (SAE-TF) as input observations. Long Short-Term Memory (LSTM) was used after CNN layers in [20] to extract the temporal features as well as other features of the PU signal to improve the detection performance. CNN-LSTM approach was also used in [21]. The authors first used a CNN to extract the energy-correlation features from the sample covariance matrix, then the output is fed to a series of LSTM layers so that the PU activity pattern can be learned, improving the detection performance further. Another architecture for SS via DL was proposed in [22] in which LSTM and CNN were used in parallel to detect modulation type and the PU signal. In [23], instead of using raw signal samples, short-time Fourier transform CNN (STFT-CNN) of samples were used as observations for training and online detection. To mention a salient work, DLSenseNet was proposed in [24] in which different CNNs along with LSTM were designed in parallel to extract spatial and temporal features of PU signal. The authors in [25] attempted to exploit Bi-LSTM and self-attention layers

Mohammad Reza Amini is with Department of Systems and Computer Engineering, Carleton University, (email: Mr.amini@ieee.org)

Ala'a Al-Habashna is with Department of Systems and Computer Engineering, Carleton University, (email: AlaaAlHabashna@cmail.carleton.ca)

Gabriel Wainer is with Department of Systems and Computer Engineering, Carleton University, (email: gwainer@sce.carleton.ca)

Gary Boudreau , Senior Member Ericsson Canada, Ottawa, ON, L4W 5K4, Canada, (email:gary.boudreau@ericsson.com)

to extract local features and global correlations for sensing the PU occupancy.

All of the mentioned structures show superiority over traditional approaches. However, they suffer from SNR-wall problem at which the detection probability decreases significantly when SNR falls below a certain threshold[1].

To make the sensing performance more robust to noise uncertainty, we propose a Multi-resolution Correlation Deep Sensing Network (MrCorr-DSNet) to sense OFDM-based signals. MrCorr-DSNet uses a signal-dependent 3 dimensional-CNN (3D-CNN) in its first layer to perform multi-scale auto-correlation in order to extract explainable features such as Cyclic Prefix (CP) similarities and signal energy as well as other non-explainable spatial and temporal features. To exploit In-phase (I) and Quadrature (Q) components of the received signal in a multi-antenna structure, each input observation is formed as a 3D matrix, providing efficient spatial-temporal feature extraction. To further improve the detection performance of MrCorr-DSNet, ensemble MrCorr-DSNet is proposed. By training several MrCorr-DSNets within different SNR sub-ranges and fusing their outputs, ensemble MrCorr-DSNet manifests its robustness to noise uncertainty, resolving the SNR-wall problem. The final structure is shown to be superior to those existing in the literature.

The main contributions of this work are summarized below.

- Designed and implemented a MrCorr-DSNet through which signal energy and CP similarities of OFDM signal as well as other non-explainable spatial and temporal features are extracted via performing multi-resolution auto-correlations
- Formed a 3D matrix for each observation by sorting the signal samples of In-phase and Quadrature from different antennas. Then, a 3D signal dependent CNN with 3D kernels is employed to fully extract the spatial-temporal correlations of OFDM signal in a multi-antenna system.
- Enhanced detection performance and resolved the SNR-wall problem by adopting ensemble learning for several MrCorr-DSNets trained for different SNR sub-ranges. By employing ensemble learning, each MrCorr-DSNet extracts fine features in SNR sub-range for which it is well-trained (acting as a strong learner) and extracting coarse features in other SNR-ranges (acting as a weak learner).

The rest of this paper is organized as follows. Section II describes the system model and the proposed DL structure. Furthermore, data set generation, offline training, online detection, and performance evaluation for MrCorr-DSNets are explained in this section. Section III discusses ensemble MrCorr-DSNets and illustrates its performance. Finally, some conclusions are provided in Section IV.

II. System Model and Problem Formulation

Consider a multi-antenna spectrum sharing scenario in which cognitive users (secondary users) co-exist with an OFDM-based primary network. Let $\mathbf{Y} = [Y_1, Y_2, \cdots, Y_M]^T$ denote the received OFDM signals at the SU receiver, where Y_m $\big(m \in \{1, \cdots, M\}\big)$ is the received signal from the m^{th} antenna. Furthermore, Y_m consists of B OFDM blocks, that is $Y_m = [Y_m^{(1)}, Y_m^{(2)}, \cdots, Y_m^{(B)}]$ in which $Y_m^{(b)}$ $\big(b \in \{1, \cdots, B\}\big)$ is the b^{th} OFDM block of Y_m. Each OFDM block of the received signal contains N_d data symbols plus N_c extra symbols as cyclic prefix, i.e.,

$$Y_m^b = [y_m^{(b)}(1), y_m^{(b)}(2), \cdots, y_m^{(b)}(N_d + N_c)]. \tag{1}$$

Note that $y_m^{(b)}(n)$ $\big(n \in \{1, 2, \cdots, N_d + N_c\}\big)$ contains I and Q components that can be extracted as $y_{m,I}^{(b)}(n) = Imag(y_m^{(b)}(n))$ and $y_{m,Q}^{(b)}(n) = Real(y_m^{(b)}(n))$. Such I and Q components can form 3D observations to be utilized later for training purpose. More specifically, $\hat{\mathbf{Y}}$ is a 3D observation vector which is defined as $\hat{\mathbf{Y}}(i, j, 1) \triangleq \mathbf{Y}_I$ and $\hat{\mathbf{Y}}(i, j, 2) \triangleq \mathbf{Y}_Q$ $\big(\forall i, j \quad i \in \{1, \cdots, M\}, j \in \{1, \cdots, B(N_d + N_c)\}\big)$. Note that by forming such a 3D vector, the deep sensing structure can fully exploit temporal and spacial correlations between different antennas, I-Q components, and signal samples. Finally, spectrum sensing is a classification problem and can be formulated as the following binary hypothesis testing problem,

$$\begin{cases} H_0: & y_m^{(b)}(n) = w_m^b(n), \\ H_1: & y_m^{(b)}(n) = \sum_{p=1}^{P} h_p x^{(b)}(n - \delta_p) + w_m^b(n), \end{cases} \tag{2}$$

where H_0 and H_1 represent the hypotheses of PU being absent and present, respectively. $w_m^b(n)$ is the complex Additive White Gaussian Noise (AWGN) with zero-mean and variance σ^2, $x^{(b)}(n-\delta_p)$ is the transmitted signal by PU, δ_p is the delay of the p^{th} multi-path component of the channel between the PU and SU, and h_p represents the channel gain of the p^{th} path which is assumed constant during the sensing process. It is assumed that there is no prior knowledge of PU signal at SU location, thus, the signal samples $x^b(n)$ can be assumed to follow an independent and identically distributed (i.i.d) circularly symmetric complex Gaussian (CSCG) with zero mean and variance σ_x^2. For a typical sensing method such as basic energy detector, the test statistic $\mathbb{T}$ is written as,

$$\mathbb{T} = \frac{1}{MB(N_d + N_c)} \sum_{m=1}^{M} \sum_{b=1}^{B} \sum_{n=0}^{N_d+N_c} |y_m^{(b)}(n)|^2. \tag{3}$$

Two performance metrics for spectrum sensing process are the probabilities of false-alarm (P_{fa}) and detection (P_d) (or equivalently miss-detection) which are described as,

$$\begin{aligned} P_{fa} &= \Pr(\mathbb{T} > \gamma \mid H_0), \\ P_d &= \Pr(\mathbb{T} > \gamma \mid H_1), \end{aligned} \tag{4}$$

where γ is the sensing threshold calculated based on the noise variance. To design a data driven test statistic, a DL approach is exploited to sense the PU occupancy instead of using traditional approaches. A general procedure for performing deep sensing is shown in Figure 1. It consists of two main steps, offline training and online detection. In the following, the mentioned steps are introduced.

[1]Cooperative SS (CSS) shows to be very robust to this problem. However, CSS might not be applicable in many communication scenarios.

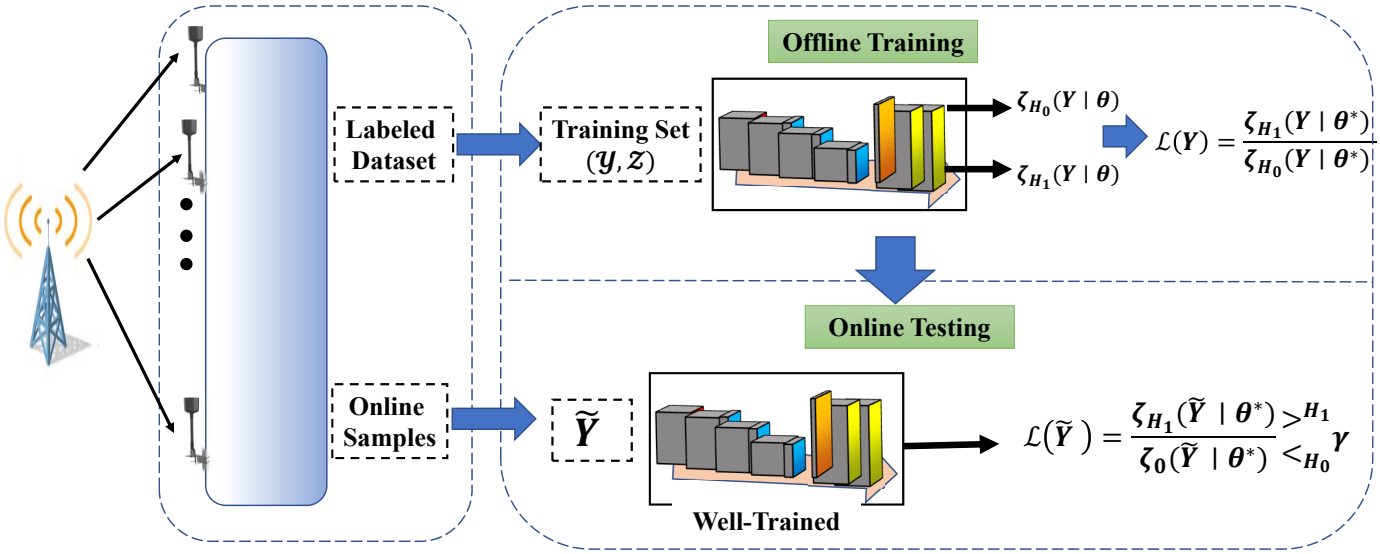

Fig. 1: General approach For Deep Sensing

A. Multi-resolution Correlation Deep Sensing Network (MrCorr-DSNet)

The main metric in spectrum sensing is the energy of the received signal. Signal energy can be extracted according to (3). To sense OFDM signal efficiently without any prior knowledge of the signal, one can think about designing a deep neural structure to extract explainable features of OFDM signal. In addition to non-explainable OFDM signal features, the proposed structure is designed to extract both the energy of the signal samples and the similarity between different parts of the observed signal. Since CP is added between OFDM symbols, extracting the similarity of different signal parts helps improve the sensing performance as the CP makes OFDM signal more distinguishable and unique from noise. Note that energy of the signal $y(n)$ can be extracted by the convolution operator ($\circledast$) as,

$$E_y = [y(n) \circledast y(-n)]_{n=0}\,. \tag{5}$$

Furthermore, cross-correlation is a measure of computing the similarity between the samples of the signals $x(n)$ and $y(n)$ (or between different parts of the same signal) which can be represented by convolution operation as,

$$\mathcal{R}_{x,y}(n) = x(n) \circledast y(-n). \tag{6}$$

In case of extracting the similarities between the signal and its parts, we exploit partial auto-correlation as,

$$\mathcal{R}_{x,x_p}(n) = x(n) \circledast x_p(-n) \tag{7}$$

where $x_p(n)$ is the part of the signal $x(n)$. Since CNNs can perform convolution operation, the question is that how they can be used to extract signal energy and the induced autocorrelation in PU signal that is a result of CP. To do this, CNNs must be modified to perform convolution operation in different scales or resolutions. Furthermore, CNN kernels must be chosen based on signal samples. Therefore, by setting CNN kernels equal to signal samples and by adopting different kernel sizes from the order of CP length to the order of whole signal duration, signal-dependent CNN is implemented, through which Multi-resolution Correlation Deep Sensing Network (MrCorr-DSNet) is achieved. Fig. 2 shows the proposed deep sensing structure. The mentioned 3D observations are firstly entered into the signal-dependent 3D-CNN and then pass through three 3D-CNNs each with ReLu activation function. For the signal-dependent CNN, four kernels are considered with different sizes that are equal to CP length[2], OFDM minimum symbol size (based on minimum FFT size), OFDM maximum symbol size (based on the maximum FFT size), and whole signal length (three OFDM symbols herein). To have the same size output, the kernels are zero-padded and the stride length is set to one for all dimensions. Its output passes through three 3D-CNNs with ReLu activation function. A batch normalization layer is used after each of the mentioned three CNNs along with a max-pooling layer for the first two. The batch normalization module removes the internal covariate shift and thus ensures a faster training process [26]. It also regularizes the structure and improves extracting local-feature. The max-pooling layer utilizes the maximum value from neuron clusters in the previous layer. This also adjusts the effect of overfitting. The flattened layer along with two fully connected (FC) layers is used after CNNs. Finally, a softmax layer is used to obtain normalized output scores. To avoid overfitting, an early stopping algorithm is employed to stop the training process if the validation loss does not decrease within 8 successive epochs. The model hyperparameters are summarized in Table I.

B. Offline Training

To train the proposed deep sensing network, the labeled samples are collected to construct the training set $(\mathcal{Y}, \mathcal{Z}) =$

[2]Usually, two sizes are defined for CP in many standards, normal CP and extended CP. Shorter is set to 10% and longer is set to 20% of OFDM symbol size

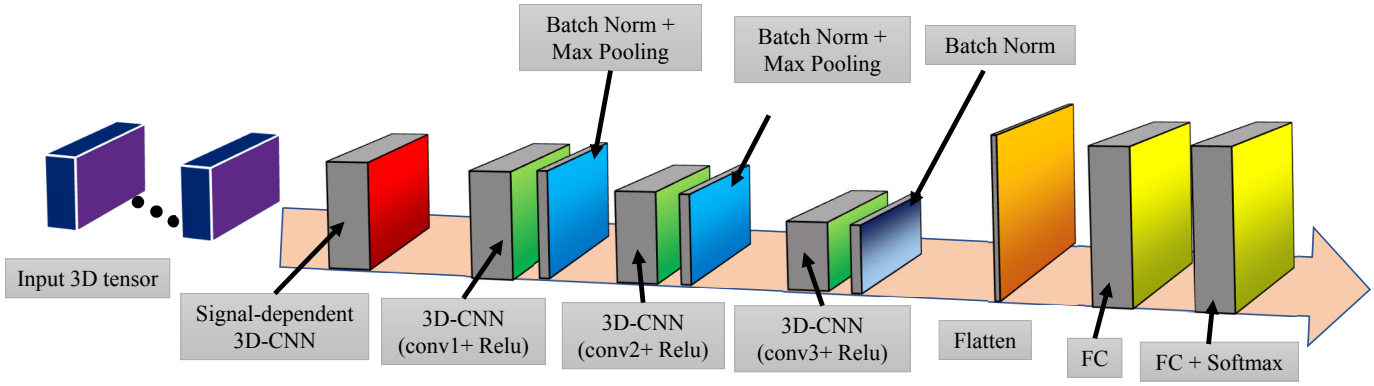

Fig. 2: The proposed structure for Deep Sensing

TABLE I: Hyperparameter Settings

Parameter	Value
MiniBatchSize	25
MaxEpochs	30
Kernel size (conv1)	$2 \times 15 \times 2$
Kernel size (conv2 & conv3)	$2 \times 3 \times 2$
# Kernels (conv1)	64
# Kernels (conv2 & conv3)	32
Optimizer	SGD
Learning rate	0.002
Max-Pooling size (first)	$1 \times 10 \times 1$
Max-Pooling size (second)	$1 \times 5 \times 1$
Stride (All CNNs)	$1 \times 1 \times 1$

$\left\{(\hat{\mathbf{Y}}^{(1)}, \mathbf{Z}^{(1)}), \cdots, (\hat{\mathbf{Y}}^{(K)}, \mathbf{Z}^{(K)})\right\}$ in which K is the total number of observations and $\mathbf{Z}^{(k)}$ belongs to the set $\{1, 0\}$ with $z = 0$ and $z = 1$ for H_0 and H_1 hypothesis, respectively. Therefore, for the classification purpose, one-hot coding is used to label output as,

$$\mathbf{Z}^{(k)} = \begin{cases} [0 \quad 1]^T & for \quad H_0, \\ [1 \quad 0]^T & for \quad H_1 \end{cases} \tag{8}$$

Correspondingly, the output of deep sensing structure for the k^{th} observation is a two-class score vector which is normalized by softmax function [27] expressed as,

$$\mathbf{Z}^{(k)} = \begin{cases} \zeta_{H_0}(\hat{\mathbf{Y}}^{(k)} \mid \theta) & for \quad H_0, \\ \zeta_{H_1}(\hat{\mathbf{Y}}^{(k)} \mid \theta) & for \quad H_1 \end{cases} \tag{9}$$

where $\zeta_{H_i}(\hat{\mathbf{Y}}^{(k)} \mid \theta) \triangleq \Pr(\hat{\mathbf{Y}}^{(k)} \mid H_i, \theta)$ and θ denotes the deep sensing model parameter. Thus, $\zeta_{H_0}(\hat{\mathbf{Y}}^{(k)} \mid \theta) + \zeta_{H_1}(\hat{\mathbf{Y}}^{(k)} \mid \theta) = 1$. Normally, the decision rule is to compare the two output scores and select the hypothesis with the maximum score which means,

$$\zeta_{H_1}(\hat{\mathbf{Y}}^{(k)} \mid \theta) \underset{H_0}{\overset{H_1}{\gtrless}} \zeta_{H_0}(\hat{\mathbf{Y}}^{(k)} \mid \theta). \tag{10}$$

However, the optimum spectrum senor is the one who consider the distribution of H_0 and H_1 in its decision, making maximum a posteriori probability estimator (MAP) rather than a Maximum Likelihood (ML) one. However, it is assumed that the prior knowledge (distributions) on PU traffic is not available. On the other hand, the training goal in spectrum sensing is to maximize the detection probability under some false-alarm constraint (the detection probability is the main metric should be met). Therefore, a threshold γ is set to give us a degree of freedom to run a trade-off between false-alarm and detection probabilities as $\mathcal{L}(\hat{\mathbf{Y}}^{(k)}) = \frac{\zeta_{H_1}(\hat{\mathbf{Y}}^{(k)}|\theta)}{\zeta_{H_0}(\hat{\mathbf{Y}}^{(k)}|\theta)} \gtrless \gamma$. The objective function for the training problem can be written as maximizing the following likelihood function [28], [29].

$$\mathbb{L}(\theta) = \prod_{k=1}^{K} \left(\zeta_{H_1}(\hat{\mathbf{Y}}^{(k)})\right)^{z^{(k)}} \left(\zeta_{H_0}(\hat{\mathbf{Y}}^{(k)})\right)^{1-z^{(k)}}. \tag{11}$$

Equivalently, based on the log likelihood function of (11), the optimization problem related to the training process can be written as the minimization of cross-entropy between the actual PU state and the output score of all observations as [29],

$$\mathbb{E}(\theta) = -\frac{1}{K}\log(\mathbb{L}(\theta)) = -\frac{1}{K}\sum_{k=1}^{K} z^{(k)} \log\left(\zeta_{H_1}\left(\hat{\mathbf{Y}}^{(k)}\right)\right) + (1 - z^k)\log\left(1 - \zeta_{H_0}\left(\hat{\mathbf{Y}}^{(k)}\right)\right). \tag{12}$$

Thus, the optimization problem is written as,

$$\theta^* = \underset{\theta}{\operatorname{argmin}} \quad \mathbb{E}(\theta) \tag{13}$$

by adopting backpropagation algorithm and Stochastic Gradient Decent (SGD) as the optimizer, the probabilities of $\zeta_{H_0}\left(\hat{\mathbf{Y}}^{(k)}\right)$ and $\zeta_{H_1}\left(\hat{\mathbf{Y}}^{(k)}\right)$ are maximized under the labels 0 and 1, respectively[3].

C. Data Set Generation

To train the proposed structure, a data set is needed. A synthesized was used in (2). For the hypothesis H_0, complex AWGN samples with zero mean and different variances have been generated. The noise variance must be set such that different SNR values according to Table II are provided. To

[3]This is equivalent to entropy minimization between the actual PU state and its score value.

generate OFDM signal, random integers according to different modulation types and modulation orders are generated. The data set is augmented with different OFDM block sizes based on different FFT sizes and CP lengths[4]. To exploit CP similarities, at least two OFDM blocks are needed as observation samples[5]. The channel is constructed as Rayleigh with random number of path delays and path gains. To generate it, delay and gain vectors are formed as shown in Table II. These vector contains 9 entries. To have a random number of delays and gains, each time a random integer between 1 and 9 is generated and some values for path delays and gains are taken out of the corresponding vectors.

TABLE II: Data set parameters

Parameter	Value
# Antenna	2
Modulation Type	PSK, QAM
Modulation Order	$[2, 4, 8, 16, 32, 64, 128, 256]$
Type of signal	In-Pahse & Quadrature
Sample length for training signals	3 OFDM Blocks
# Observations (Training +Validation)	108360
Validation Ratio	30%
SNR Range (dB)	[-15, 0] (step size 0.2)
CP length	8% & 25% of OFDM symbol
FFT Size	[64, 128, 256, 512, 1024, 2048, 4096]
Path Gain Vector (dB)	[0, -1.5, -2.5, -3.5, -0.6, -9, -7, -12, -16]
Path Delay Vector (Sec)	[0, 30, 150, 310, 370, 710, 1090, 1730, 2510]*1e-9

D. Online Detection

After achieving the optimum parameter values (θ^*) in (13) by SGD through backpropagation, the proposed structure is well-trained. For online detection, the structure must be fine-tuned according to the spectrum sensing performance metrics. Since the last layer (softmax) outputs two score values for H_0 and H_1, one simple decision is to compare these two scores and decide on the PU occupancy state according to the maximum output. However, to provide a degree of freedom to run a trade-off between P_{fa} and P_d, a ratio $\mathcal{L}(\hat{\mathbf{Y}}^{(k)}) = \frac{\zeta_{H_1}(\hat{\mathbf{Y}}^{(k)}|\theta^*)}{\zeta_{H_0}(\hat{\mathbf{Y}}^{(k)}|\theta^*)}$ is calculated according to Neyman-Pearson theorem[6] and is compared with a detection threshold γ. Such a threshold can be determined using the Monte Carlo method for a target P_{fa} value. To choose a threshold value, empirical P_{fa} is calculated based on the obtained $\mathcal{L}(\hat{\mathbf{Y}}^{(k)})$ under optimum parameters θ^* and H_0 hypothesis. More specifically, $\mathcal{L}(\hat{\mathbf{Y}}^{(k)};\theta^*)$ for all observations under the hypothesis H_0 is sorted in a descending order. Denoting $\hat{\mathbf{Y}}_s^{(l)}$ as the l^{th} element of the sorted observation set and assuming that the total number of observations under H_0 hypothesis is N_{H_0} then the detection threshold is obtained as,

$$\gamma = \mathcal{L}\left(\hat{\mathbf{Y}}_s^{(k)}\lfloor \delta_{fa} N_{H_0} \rfloor; \theta^*\right) \tag{14}$$

where δ_{fa} is the false-alarm target value, i.e., $P_{fa} \leq \delta_{fa}$. Upon collecting online samples $\hat{\mathbf{Y}}_{online}$, they are fed into the proposed structure to obtain the two score values. Then, the decision is made as,

$$\mathcal{L}(\hat{\mathbf{Y}}_{online}) \underset{H_0}{\overset{H_1}{\gtrless}} \gamma \tag{15}$$

E. Performance Evaluation of MrCorr-DSNet

To evaluate the performance of the proposed MrCorr-DSNet, the model must be trained and validated before online testing. Figs. 3 and 4 show the proposed network accuracy and loss for both training and validation data, respectively. As can be seen, the accuracy increases during the training process and reaches the final value of 96%. Starting from 1, the loss value decreases until it finds the final value of almost 0.1.

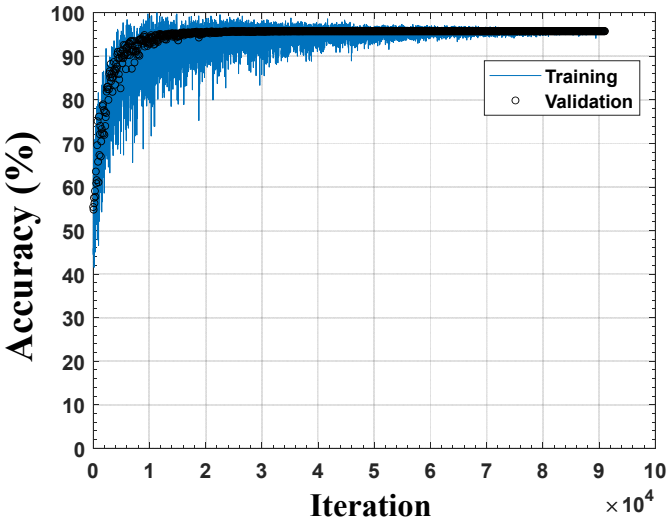

Fig. 3: Training and validation accuracy of MrCorr-DSNet vs. the number of iterations.

The probability of detection versus SNR for the MrCorr-DSNet along with the most recent proposed structures in the literature– namely CNN-LSTM [21], Detect-Net [20], and DLSenseNet [24]– are plotted in Fig. 5. For fair comparison, numerous simulations are performed for each model to find the best hyperparameters. As can be seen, the proposed MrCorr-DSNet achieves better detection performance than the others. The proposed structure even outperforms other models by achieving lower P_f. Particularly, the corresponding false-alarm probabilities calculated after the training process are $P_f(\text{CNN-LSTM}) = 7.2\%$, $P_f(\text{DetectNet}) = 5.6\%$, $P_f(\text{DLSenseNet}) = 3.4\%$, $P_f(\text{MrCorr-DSNet}) = 2.3\%$

Interestingly, it is observed that MrCorr-DSNet has shifted the SNR-wall down to -4dB which is 2 dB lower than other models. Another observation is that the rate at which the detection probability decreases for low SNRs is lower than that of other models. This causes P_d to be higher than 80% for

[4]We used popular FFT size and CP length for OFDM communication scenarios such as 5G, LTE, IEEE802.11, and IEEE802.16.

[5]This is because no synchronization between secondary and primary networks is assumed. Here we used three OFDM blocks.

[6]Since the prior distribution of the two Hypothesis obtained during the training process is not optimum to be used in online detection, likelihood ratio is applicable according to defined $\mathcal{L}(\hat{\mathbf{Y}}^{(k)})$.

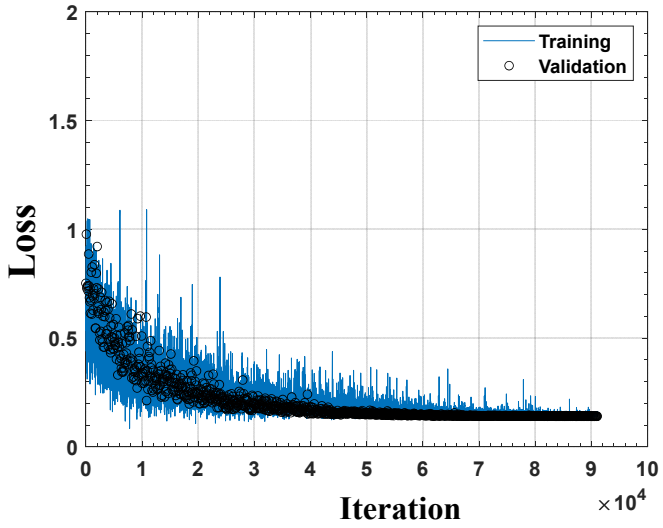

Fig. 4: Training and validation loss for MrCorr-DSNet vs. umber of iterations.

SNR ≥ -9 dB. This is due to the fact that the proposed structure is semi-blind since it exploits the CP similarities of OFDM signals. Although the detection performance of MrCorr-DSNet is superior to other models, it is still low under medium noise uncertainty. For instance, $P_d = 71\%$ and $P_d = 62\%$ under SNR=-12 dB and SNR=-15 dB, respectively. In next section, the performance of the proposed model is significantly improved by employing ensemble learning.

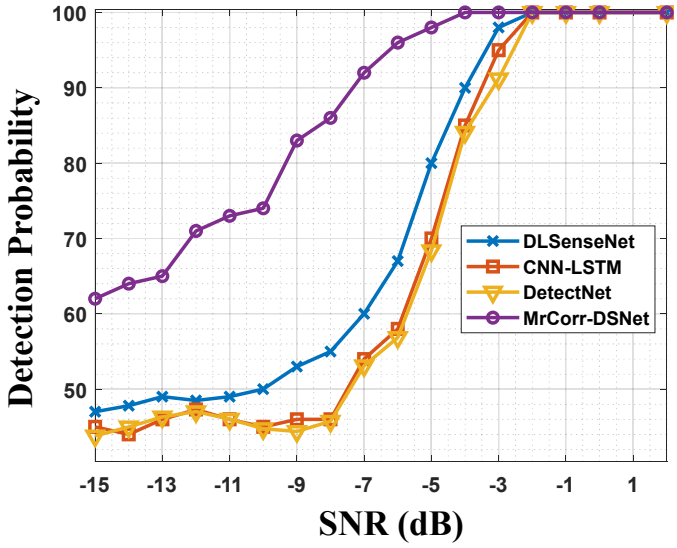

Fig. 5: Detection probability vs. SNR.

III. Ensemble Deep Spectrum Sensing

A. Ensemble Structure

In the previous section, a deep sensing network based on multi resolution correlation concept to extract explainable features from OFDM signals was proposed. Results showed that the proposed architecture outperformed other state-of-the-art solutions. Although the final validation accuracy of 96% was achieved, similar to the existing structures in the literature and due to the SNR-wall limitation, the performance of the proposed structure is still low under high noise uncertainty[7]. As an example, for the underlying data set, the accuracy at -15 dB is 62% and 48% for MrCorr-DSNet and DLSenseNet, respectively. After performing extensive simulations, we found the reason for this phenomenon. Since MrCorr-DSNet and others are trained for a wide range of SNR simultaneously, the networks are failed to extract fine features for the worst cases of observations, i.e., signals with very low energy (low SNR). Indeed, CNNs tend to learn features for some straightforward observations. The problem will not be resolved even by increasing the number of CNN filters, which would only make the structure more complex. Therefore, the solution is to have different MrCorr-DSNets for different SNR sub-ranges. In such a way, each MrCorr-DSNet extracts fine features in SNR sub-range for which it is well-trained (acting as a strong learner) and extracting coarse features in other SNR-ranges (acting as a weak learner). Hence, there exist several models and the final decision is made by fusing their outputs. This guides the final structure toward ensemble learning. Random forest is selected to combine the output of parallel MrCorr-DSNet with 6 SNR sub-ranges. The number of learning cycles is 100 and the ensemble aggregation method is bagging.

B. Performance Evaluation of ensemble MrCorr-DSNet

The performance of the ensemble structure is evaluated and compared with MrCorr-DSNet and other structures in the literature. Ensemble MrCorr-DSNet is evaluated based on different metrics such as, confusion matrix, Area Under Curve (AUC) , P-Value, loss, ROC and detection probability for different SNRs. Fig. 6 shows the confusion matrix for both MrCorr-DSNet and ensemble MrCorr-DSNet. As can be seen, detection probability improves from 93.1% to 98.8% by training MrCorr-DSNet for different SNR sub-ranges and employing random forest as ensemble method. There is a slight reduction in false-alarm probability from 2.3% to 2.0%. This is because scores related to H_1 are considered as the input of ensemble structure.

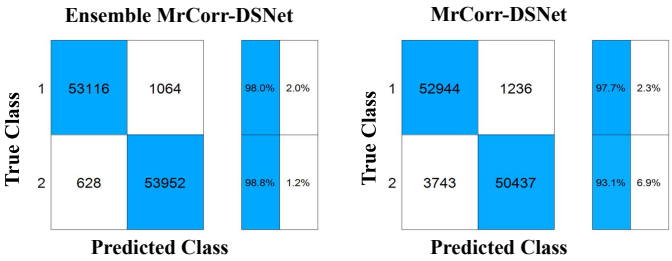

Fig. 6: Confusion Matrix for both MrCorr-DSNet and ensemble MrCorr-DSNet.

Furthermore, Loss, P-Value, and AUC for MrCorr-DSNet and ensemble MrCorr-DSNet is compared in Table III. It is observed that employing ensemble strategy decreases loss by

[7]Note that cooperative sensing structures are shown to have a very low SNR-wall. However, cooperative spectrum sensing is not the case in this work.

10 fold. The AUC also increases from 0.9680 to 0.9899. However, P-Value for both structures is zero.

TABLE III: Comparison of MrCorr-DSNet and ensemble MrCorr-DSNet

DL Structure	Loss	P-Value	AUC
MrCorr-DSNet	0.1192	0	0.9680
Ensemble MrCorr-DSNet	0.0101	0	0.9899

To investigate the performance of the ensemble structure, the detection probability versus SNR is plotted in Fig. 7. It is observed that in ensemble MrCorr-DSNet, the detection probability deceases at very lower rate when when the SNR decreases, staying above MrCorr-DSNet and significantly standing out of those in the literature. For instance, the detection performance is 94.4% at -15dB which is remarkably above that of the other solutions.

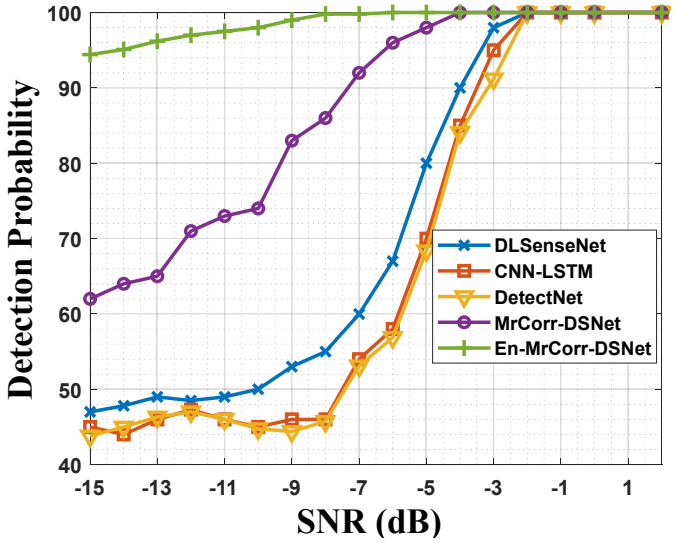

Fig. 7: Detection probability vs. SNR.

The detection performance of the ensemble MrCorr-DSNet is explored for different number of SNR sub-ranges in Fig. 8. The SNR interval for each cases is listed in IV.

TABLE IV: SNR interval for different number of sub-ranges

# SNR sub-ranges	Sub-range Intervals (dB)
1	[2,-15]
2	[2,-6.4] , [-6.6, -15]
4	[2,-2], [-2.2, -6.4], [-6.6, -10.8], [-11,-15]
6	[2,-1], [-1.2,-4], [-4.2,-7], [-7.2, -10] [-10.2, -13], [-13.2,-15]
8	[2,0], [-0.2,-2.4], [-2.6,-4], [-4.2, -6.2] [-6.4, -8.6], [-8.8,-10.8], [-11,-13], [-13.2, -15]

The lowest performance under high noise uncertainty is for MrCorr-DSNet that is trained under one SNR sub-range. As can be seen, the higher the number of sub-ranges, the better the detection probability. However, the performance of the structure seems to converge when the number of sub-ranges increases.

Fig. 9 shows the ROC curve for MrCorr-DSNet and ensemble MrCorr-DSNet. Employing ensemble structures within different SNR sub-ranges helps improve the ROC for ensemble MrCorr-DSNet and makes it superior to MrCorr-DSNet.

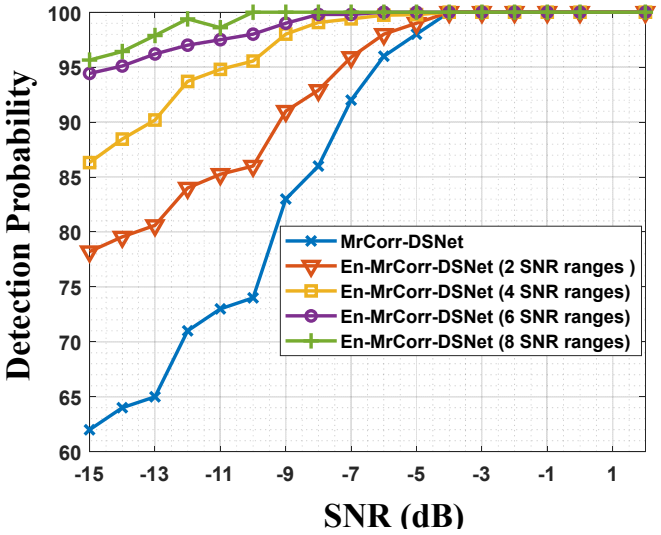

Fig. 8: Detection probability for different number of SNR sub-ranges vs. SNR.

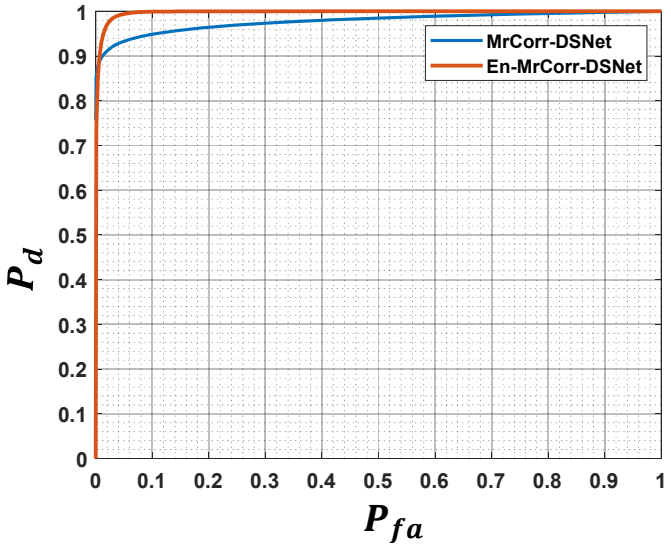

Fig. 9: ROC curve for both MrCorr-DSNet and ensemble MrCorr-DSNet.

IV. Conclusions

A multi-resolution Correlation Deep Sensing Network (MrCorr-DSNet) was designed and implemented in this paper to capture the signal energy and Cyclic Prefix similarities in OFDM-based signals as well as other non-explainable spatial-temporal features. Furthermore, a 3D matrix for each observation was formed by using In-phase and Quadrature components of OFDM signals in a multi-antenna scenario, helping MrCorr-DSNet fully exploit the temporal-spatial correlations among received samples. Furthermore, by adopting ensemble learning for several MrCorr-DSNets trained for different SNR sub-ranges, the detection performance was significantly enhanced and the SNR-wall problem was resolved. The final structure shows significant performance in terms of detection probability under noise uncertainty, Area Under Curve (AUC),

confusion matrix, final validation loss, and receiver operating characteristic (ROC).

ACKNOWLEDGEMENT

This work is funded by Ericsson Canada and the Natural Sciences and Engineering Research Council of Canada (NSERC).

REFERENCES

[1] D. Cabric, S. Mishra, and R. Brodersen, "Implementation issues in spectrum sensing for cognitive radios," in *Conference Record of the Thirty-Eighth Asilomar Conference on Signals, Systems and Computers, 2004.*, vol. 1, 2004, pp. 772–776 Vol.1.

[2] J. Mitola and G. Maguire, "Cognitive radio: making software radios more personal," *IEEE Personal Communications*, vol. 6, no. 4, pp. 13–18, 1999.

[3] M. R. Amini, M. Mahdavi, and M. J. Omidi, "Coexisting with the dynamic pu, the effect of pu-returns on a secondary network," *International Journal of Communication Systems*, vol. 30, no. 15, p. e3316, 2017, e3316 IJCS-16-0674.R2. [Online]. Available: https://onlinelibrary.wiley.com/doi/abs/10.1002/dac.3316

[4] M. R. Amini and M. W. Baidas, "Performance analysis of urll energy-harvesting cognitive-radio iot networks with short packet and diversity transmissions," *IEEE Access*, vol. 9, pp. 79 293–79 306, 2021.

[5] M. R. Amini, F. Hemati, and A. Mirzavandi, "Trilateral tradeoff of sensing, transmission, and contention times in a multiuser split-phase CR networks," *IEEE Sensors Journal*, vol. 15, no. 10, pp. 6044–6055, Oct. 2015.

[6] A. Al-Habashna, O. A. Dobre, R. Venkatesan, and D. C. Popescu, "Cyclostationarity-based detection of lte ofdm signals for cognitive radio systems," pp. 1–6, 2010.

[7] A. Al-Habashna, O. A. Dobre, R. Venkatesan, and Popescu, "Wimax signal detection algorithm based on preamble-induced second-order cyclostationarity," pp. 1–5, 2010.

[8] A. Al-Habashna, O. A. Dobre, R. Venkatesan, and D. C. Popescu, "Second-order cyclostationarity of mobile wimax and lte ofdm signals and application to spectrum awareness in cognitive radio systems," *IEEE Journal of Selected Topics in Signal Processing*, vol. 6, no. 1, pp. 26–42, 2012.

[9] F. Salahdine, H. E. Ghazi, N. Kaabouch, and W. F. Fihri, "Matched filter detection with dynamic threshold for cognitive radio networks," in *2015 International Conference on Wireless Networks and Mobile Communications (WINCOM)*, 2015, pp. 1–6.

[10] P. Pandya, A. Durvesh, and N. Parekh, "Energy detection based spectrum sensing for cognitive radio network," in *2015 Fifth International Conference on Communication Systems and Network Technologies*, 2015, pp. 201–206.

[11] W. Wu, Z. Wang, L. Yuan, F. Zhou, F. Lang, B. Wang, and Q. Wu, "Irs-enhanced energy detection for spectrum sensing in cognitive radio networks," *IEEE Wireless Communications Letters*, vol. 10, no. 10, pp. 2254–2258, 2021.

[12] M. Amini and A. Mirzavandi, "Phase-type model spectrum sensing for cognitive radios," *IETE Journal of Research*, vol. 61, no. 5, pp. 510–516, 2015. [Online]. Available: https://doi.org/10.1080/03772063.2015.1024177

[13] Y. Zeng, C. L. Koh, and Y.-C. Liang, "Maximum eigenvalue detection: Theory and application," in *2008 IEEE International Conference on Communications*, 2008, pp. 4160–4164.

[14] Y. Zeng and Y.-C. Liang, "Spectrum-sensing algorithms for cognitive radio based on statistical covariances," *IEEE Transactions on Vehicular Technology*, vol. 58, no. 4, pp. 1804–1815, 2009.

[15] M. R. Amini, M. Moghadasi, and I. Fatehi, "A bfsk neural network demodulator with fast training hints," in *2010 Second International Conference on Communication Software and Networks*, 2010, pp. 578–582.

[16] A. Felix, S. Cammerer, S. Dörner, J. Hoydis, and S. Ten Brink, "Ofdm-autoencoder for end-to-end learning of communications systems," in *2018 IEEE 19th International Workshop on Signal Processing Advances in Wireless Communications (SPAWC)*, 2018, pp. 1–5.

[17] Y. Liu, Y. Li, Y. Zhu, Y. Niu, and P. Jia, "A brief review on deep learning in application of communication signal processing," in *2020 IEEE 5th International Conference on Signal and Image Processing (ICSIP)*, 2020, pp. 51–54.

[18] L. Liu, M. Sheng, J. Liu, Y. Dai, and J. Li, "Stable throughput region and average delay analysis of uplink NOMA systems with unsaturated traffic," *IEEE Transactions on Communications*, vol. 67, no. 12, pp. 8475–8488, 2019.

[19] Q. Cheng, Z. Shi, D. N. Nguyen, and E. Dutkiewicz, "Sensing ofdm signal: A deep learning approach," *IEEE Transactions on Communications*, vol. 67, no. 11, pp. 7785–7798, 2019.

[20] J. Gao, X. Yi, C. Zhong, X. Chen, and Z. Zhang, "Deep learning for spectrum sensing," *IEEE Wireless Communications Letters*, vol. 8, no. 6, pp. 1727–1730, 2019.

[21] J. Xie, J. Fang, C. Liu, and X. Li, "Deep learning-based spectrum sensing in cognitive radio: A cnn-lstm approach," *IEEE Communications Letters*, vol. 24, no. 10, pp. 2196–2200, 2020.

[22] M. Xu, Z. Yin, M. Wu, Z. Wu, Y. Zhao, and Z. Gao, "Spectrum sensing based on parallel cnn-lstm network," in *2020 IEEE 91st Vehicular Technology Conference (VTC2020-Spring)*, 2020, pp. 1–5.

[23] Z. Chen, Y.-Q. Xu, H. Wang, and D. Guo, "Deep stft-cnn for spectrum sensing in cognitive radio," *IEEE Communications Letters*, vol. 25, no. 3, pp. 864–868, 2021.

[24] S. Solanki, V. Dehalwar, and J. Choudhary, "Deep learning for spectrum sensing in cognitive radio," *Symmetry*, vol. 13, no. 1, 2021. [Online]. Available: https://www.mdpi.com/2073-8994/13/1/147

[25] H. Xing, H. Qin, S. Luo, P. Dai, L. Xu, and X. Cheng, "Spectrum sensing in cognitive radio: A deep learning based model," *Transactions on Emerging Telecommunications Technologies*, vol. 33, no. 1, p. e4388, 2022. [Online]. Available: https://onlinelibrary.wiley.com/doi/abs/10.1002/ett.4388

[26] J. Wang, S. Li, Z. An, X. Jiang, W. Qian, and S. Ji, "Batch-normalized deep neural networks for achieving fast intelligent fault diagnosis of machines," *Neurocomputing*, vol. 329, pp. 53–65, 2019. [Online]. Available: https://www.sciencedirect.com/science/article/pii/S0925231218312384

[27] M. Jiang, Y. Liang, and X. Feng, "Text classification based on deep belief network and softmax regression," *Neural Computing and Applications*, vol. 29, no. 1, pp. 61–70, 2018.

[28] J. Schmidhuber, "Deep learning in neural networks: An overview," *Neural Networks*, vol. 61, pp. 85–117, 2015. [Online]. Available: https://www.sciencedirect.com/science/article/pii/S0893608014002135

[29] C. Liu, J. Wang, X. Liu, and Y.-C. Liang, "Deep cm-cnn for spectrum sensing in cognitive radio," *IEEE Journal on Selected Areas in Communications*, vol. 37, no. 10, pp. 2306–2321, 2019.